Electronic Supplementary Material (ESI) for Soft Matter

A Transient Polymorph Transition of 4-Cyano-4'-octyloxybiphenyl (8OCB) Revealed by Ultrafast Differential Scanning Calorimetry (UFDSC)

Jing Jiang [†], Evgeny Zhuravlev [§], Zijie Huang[†], Lai Wei[†], Qin Xu[†], Meijuan Shan[†], Gi Xue[†], Dongshan Zhou*[,†], Christoph Schick*[,†,§], Wei Jiang*[,†,‡]

[†] Department of Polymer Science and Engineering, School of Chemistry and Chemical Engineering, State Key Laboratory of Coordination Chemistry, Nanjing University, Nanjing, 210093 China

[‡] State Key Laboratory of Pollution and Resource Reuse, School of the Environment, Nanjing University, Nanjing 210023, China

[§] Institute of Physics, University of Rostock, 18051 Rostock, Germany

Table of contents

Supporting Information

SI.1 Instrumentation and sampling

The ultrafast differential fast scanning calorimeter (UFDSC) is able to perform heat flow measurements during controlled heating or cooling up to 500,000 K/s. The experiments in this paper were performed using the sensor XI39395 with a 6-junction thermopile and a single heater. The sensor consists of a sub micron SiN_x membrane supported by a silicon frame. The heater and the hot junctions of the thermopile are located in the membrane center. All electrical connection wires are covered by an additional SiO_2 layer for electrical isolation and protection. More details about the instrument and data treatments can be found elsewhere.[1, 2]

The 8OCB sample (secondary standard for DSC temperature calibration[3]) were offered by Merck KGaA, Germany, and used as received. Its chemical structure is shown as followed.

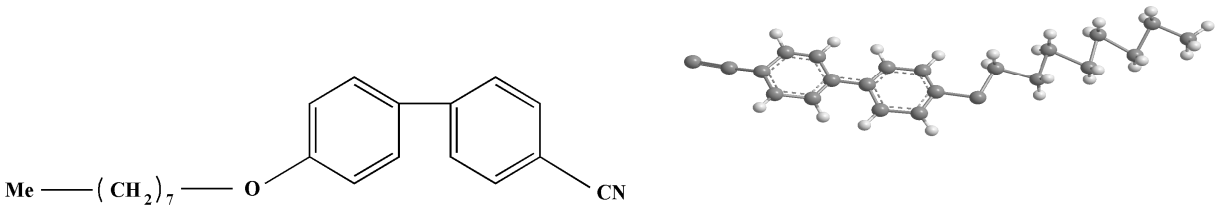

The sample was cut into a tiny grain of 15 μm×15 μm×2 μm (~5 ng) and moved onto the center of the sensor under a microscope. Then an electric pulse was applied to the heater to melt the sample and the sample became pancake-like with a thickness of about 1.5 μm. This guarantees good thermal contact between the sample and the sensor, and small temperature gradients across the sample, as shown in Figure S1.

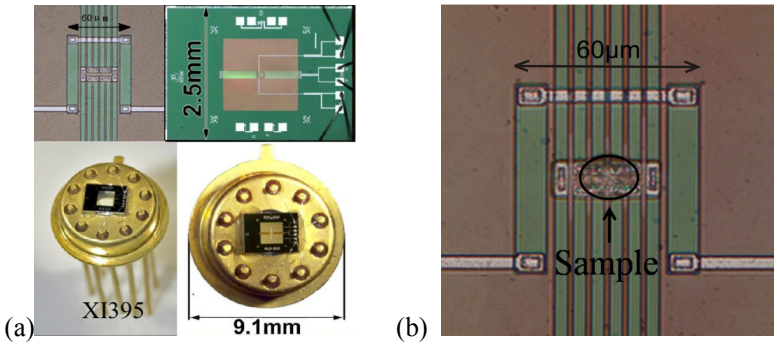

(a) (b)

FIG.S1. (a) Thin film chip sensor based on a thin free standing SiN_x film on a silicon frame and measuring area of 60 μm × 70 μm in the center of the film. (b) Photomicrograph of the sample loaded sensor XI395 (about 5 ng 8OCB).

SI. 2 Performance check of the calorimeter

We checked the scanning rate performance of the calorimeter with two empty XI395 sensors. When the scanning rate is faster than 100,000 K/s,[4] we need to use the even smaller sensor XI394 which has a smaller addenda heat capacity and smaller response time.

As shown in Figure S2, we can get well controlled cooling rates up to 20,000 K/s till 175 K which is about 50 K below the glass transition temperature of 8OCB (T_g = 230 K).

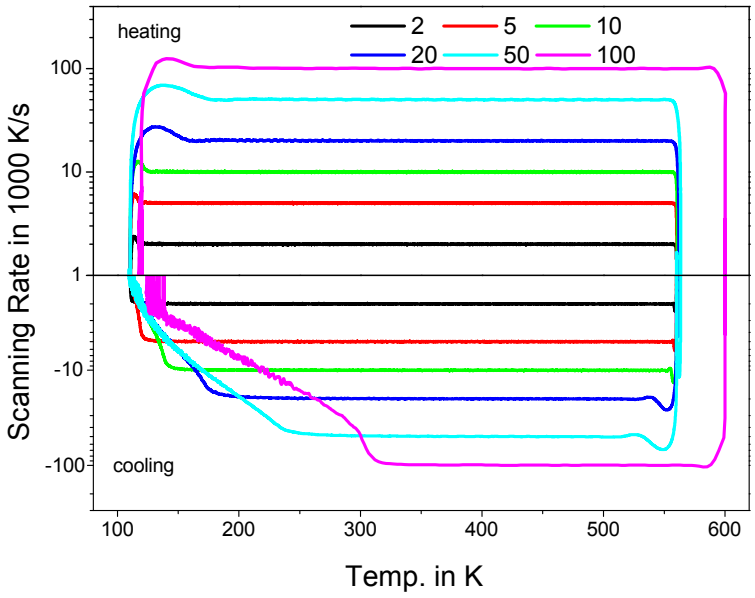

FIG.S2. Performance check of the calorimeter. Scanning rates from 2000 K/s to 100,000 K/s *vs.* temperature.

SI.3 Thermal history

First, the influence of cooling rate on the structure formation was studied at subsequent heating scans at a constant rate of 2000 K/s or 20,000 K/s. The scheme of the experiment is shown in Fig. S3.

The sample was heated to 380 K and hold there for 0.01 s to erase the thermal history and then cooled down to 110 K at different rates between 800 and 20,000 K/s. The heating scans after different cooling were either performed at 2000 K/s or 20,000 K/s.

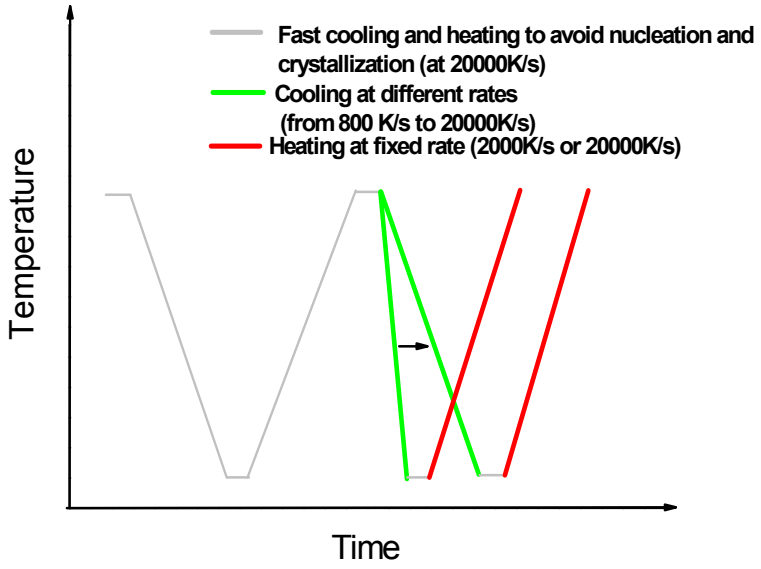

FIG.S3. Temperature-time profile for the experiment for the study of the influence of cooling rate.

Small differences between the smectic glasses obtained by cooling at different rates can be investigated by subsequent heating measurements. To check this, 8OCB was first cooled with rates from 800 K/s to 20000 K/s to sub-T_g and reheated with always the same rate of 2000 K/s. But as shown in Figure S4, 8OCB shows almost the same behavior during heating at 2000 K/s, irrespectively of the previous cooling rate. This implies that either 800 K/s' cooling is fast enough that further increasing cooling rate makes no difference, or that a heating rate of 2000 K/s is too slow to avoid reorganization before the structural transitions of 8OCB occur on heating.

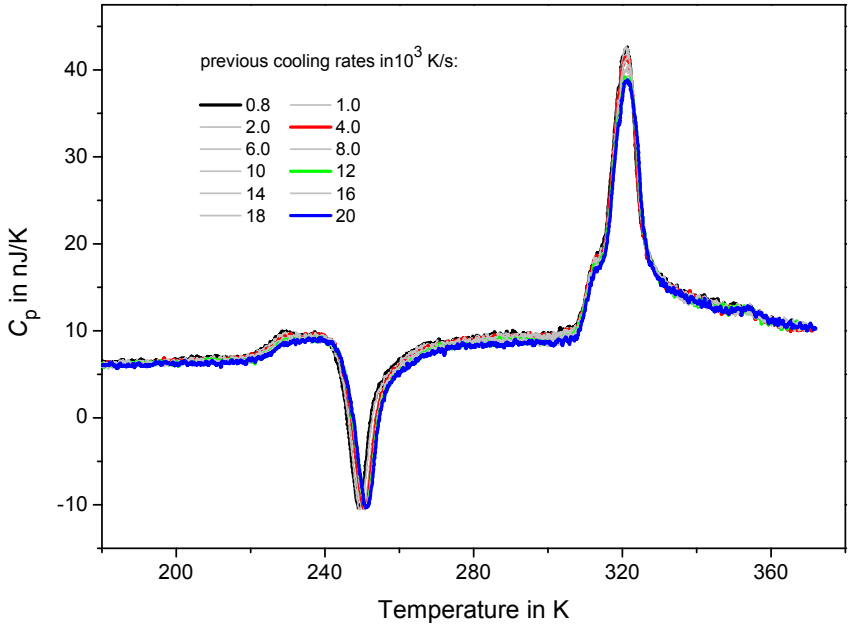

FIG.S4. Heating curves at 2000 K/s of 8OCB quenched from the melt with different cooling rates (from 800 K/s to 20,000 K/s) in the UFDSC.

Comparison with heating curves at 20,000K/s (Figure 3 in the main text), reveal the effect of previous cooling rate on the crystallization and melting behavior of 8OCB. Confirming that heating at 2000 K/s is too slow to capture the cooling history of 8OCB on heating. More importantly, at a heating rate of 20,000 K/s, the sample shows a strong cooling rate dependent cold-crystallization and melting behavior. Finally, the sample cooled with a rate of 20,000 K/s or faster basically shows no crystallization or melting. This assures that with a cooling rate of 20,000 K/s, we can obtain an apparently nuclei free smectic glass and that any crystallization observed occurs only during heating.

The main set of experiments was therefore performed in the following way: The sample was cooled so fast (20,000 K/s) that no homogeneous nucleation occurs. Then the sample was reheated at different rates between 1000 K/s and 20,000 K/s to study the transformations between different polymorphs during the heating scan. The scheme of the experiments is shown in Figure S5.

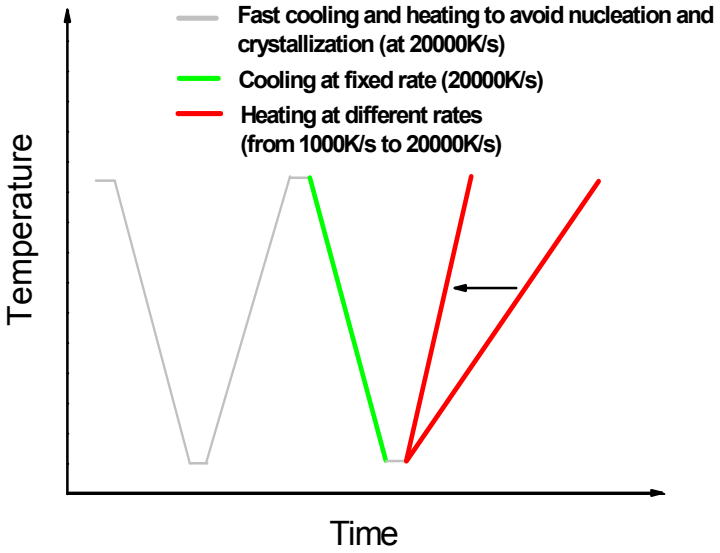

FIG.S5. Temperature-time profiles for the study of the transformation during heating.

The results of these sample treatments are discussed in the main text.

SI.4 Morphologies from microscopy and XRD patterns of different forms of 8OCB

Crystal of 8OCB have been grown from an acetone-water or a diethyl ether-methanol solution by slow evaporation of the solvents as described by Hori[5]. Crystal morphologies are shown in the micrographs of Figure S6.

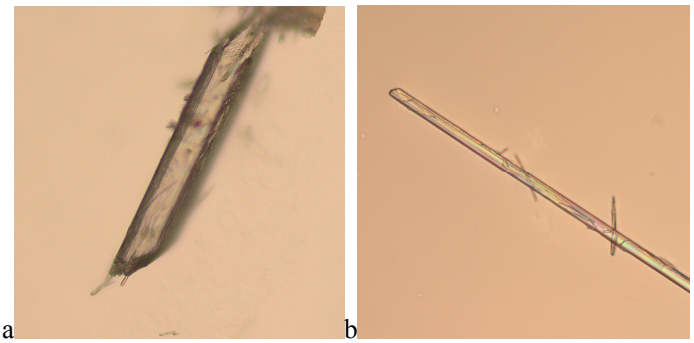

FIG.S6. a) Morphology of the long parallelepiped (PP) crystal form of 8OCB grown from acetone-water solution at fast evaporation. b) Morphology of the needle crystal (N) form of 8OCB grown from acetone-water solution with slower evaporation.

Powder X-ray scattering studies also have been carried out to obtain structural information on different phases of 8OCB. Figure S7 shows WAXS patterns for the needle and the most stable (commercially available powder specimen) crystalline forms of 8OCB at room temperature. All samples are powders crystallized from acetone-water solutions with different evaporation rates. The sample containing the needle form (N) is mixed with CP form crystals. In Figure S7, several peaks assigned as strong reflections of the CP form have been designated based on the unit cell parameters of the

CP form of 8OCB reported by Hori.[6] For the needle phase (N) a triclinic crystal structure has been reported[6] and the peaks corresponding to N are shown in the WAXS patterns (marked by *).

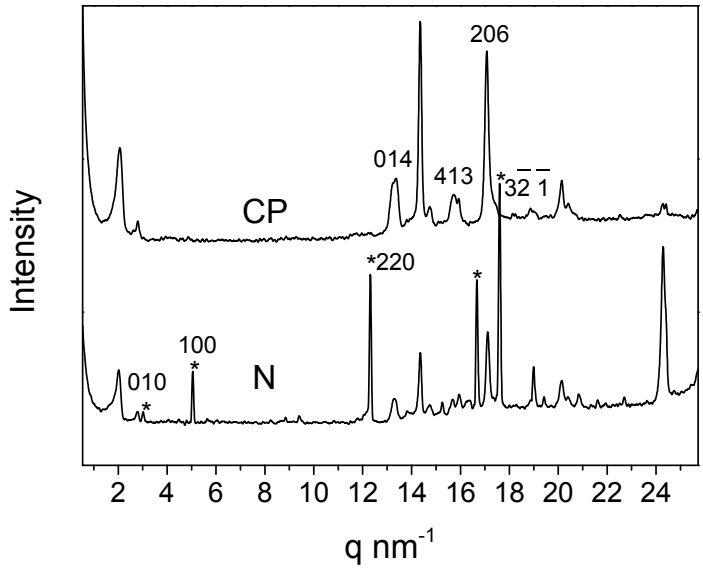

FIG.S7. WAXS patterns of CP and mixture of N and CP of 8OCB. hkl's are shown above the peaks. * denote peaks corresponding to the N form.

For PP, the single crystals grown from solution are too small to give reliable XRD patterns. The XRD patterns of the sample grown either from acetone-water or diethyl ether-methanol solution are dominated by the CP form. According to the WAXS patterns of 8OCB in a heating experiment reported by Yang et al., the peaks at 2.06 and 2.79 nm^{-1} , see Figure S8, may be related to a metastable crystal form, which could be the parallelepiped crystal or a new phase as Yang suggests.[7]

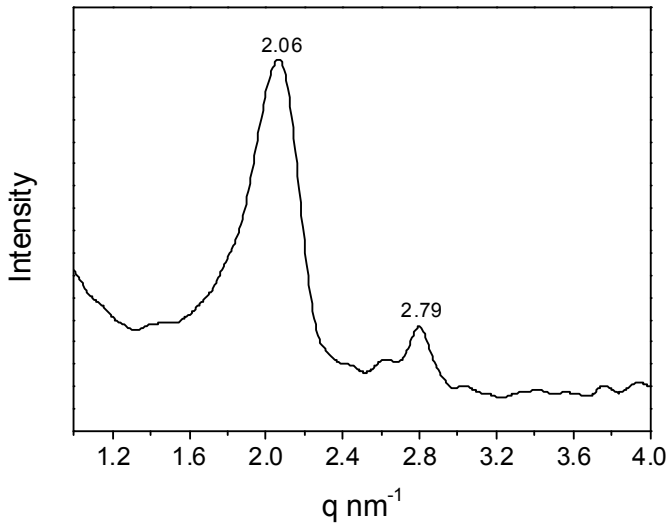

FIG.S8. WAXS pattern of 8OCB showing the peaks at 2.06 and 2.79 nm^{-1}.

SP form of 8OCB is so unstable that we can not get single crystals for the XRD experiment. The possible packing of 8OCB in the SP form is shown in Figure S9. It is constructed from that of 7OCB or 9OCB[5].

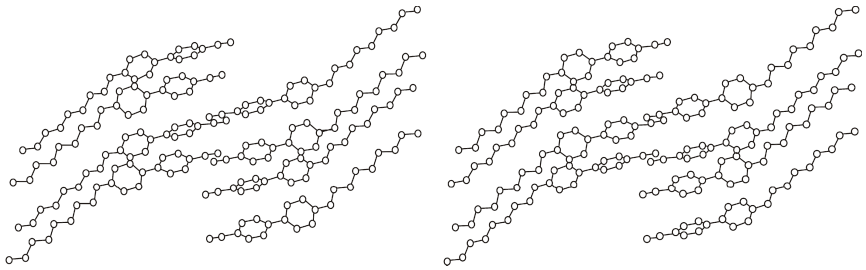

FIG.S9. Different views of the possible packing of the square-plate crystal of 8OCB.

References

1. E. Zhuravlev and C. Schick, *Thermochimica Acta*, **505**, 1.
2. E. Zhuravlev and C. Schick, *Thermochimica Acta*, **505**, 14.
3. S. M. Sarge, G. W. H. Hohne, H. K. Cammenga, W. Eysel and E. Gmelin, *Thermochim. Acta*, 2000, **361**, 1.
4. A. A. Minakov, A. W. van Herwaarden, W. Wien, A. Wurm and C. Schick, *Thermochim. Acta*, 2007, **461**, 96.
5. K. Hori and H. P. Wu, *Liq. Cryst.*, 1999, **26**, 37.
6. K. Hori, Y. Iwai, M. Yano, R. Orihara-Furukawa, Y. Tominaga, E. Nishibori, M. Takata, M. Sakata and K. Kato, *Bull. Chem. Soc. Jpn.*, 2005, **78**, 1223.
7. I. K. Yang and C. Y. Liu, *Mol. Cryst. Liquid Cryst.*, 2009, **503**, 32.